# Vacuum ultraviolet argon excimer production by use of an ultrashort-pulse high-intensity laser

Masanori Kaku,* Takeshi Higashiguchi, Shoichi Kubodera,† and Wataru Sasaki
*Department of Electrical and Electronic Engineering and Photon Science Center, Miyazaki University, Gakuen Kibanadai Nishi 1-1, Miyazaki 889-2192, Japan*
(Received 16 March 2003; published 7 August 2003)

We report on the observation of $Ar_2^*$ emission at 126 nm by use of a hollow fiber to guide the high-intensity laser propagation in high-pressure Ar. A small-signal gain coefficient of 0.05 $cm^{-1}$ was measured at 126 nm by this method. The increase of the $Ar_2^*$ emission intensity was measured to be exp(2.5), with an increase of the fiber length up to 50 cm. Kinetic analysis revealed that the $Ar_2^*$ production processes were initiated by the electrons produced by the high-intensity laser through an optical-field-induced ionization (OFI) process. A rapid conductive cooling of the OFI electrons is favorable to initiate the $Ar_2^*$ formation kinetics more efficiently. This high-density cold plasma production method should be applicable for other vacuum ultraviolet rare-gas excimer lasers.

DOI: 10.1103/PhysRevA.68.023803 PACS number(s): 42.55.Lt, 33.20.Ni

## I. INTRODUCTION

Practical short wavelength lasers in the vacuum ultraviolet (VUV) and soft x-ray spectral regions have been desired in various scientific fields. As a result of successful control of an optical-field-induced ionization (OFI) plasma produced by a high-intensity laser [1,2] and of a capillary discharge plasma driven by a compact discharge device [3], short wavelength lasers in the soft x-ray region have become more practical and compact than ever. Development of such compact soft x-ray lasers will stimulate other robust excitation methods [4,5]. Short wavelength lasers in the VUV spectral region are also in high demand, which are now used even in industrial application fields. Compact VUV lasers as well as tabletop soft x-ray lasers would be applicable for photochemistry, biological science, and new types of materials processing, since these lasers produce high-energy photons with high photon flux. There are, however, very few short wavelength lasers available that are robust enough for applications. Currently available practical VUV lasers are ArF and $F_2$ lasers at 193 and 157 nm, respectively, both of which are operated by a compact discharge device with a high repetition rate.

In addition to these VUV lasers, there are rare-gas excimer lasers, which are known to be one of the few high-power VUV lasers [6,7]. Their center wavelengths are 126, 147, and 172 nm for $Ar_2^*$, $Kr_2^*$, and $Xe_2^*$, respectively. From the practical point of view, these wavelengths are long enough to utilize transmission optics such as $MgF_2$ or LiF. Recently, a practical compact $Kr_2^*$ laser was first demonstrated by use of discharge excitation by our group [8]. Among these rare-gas excimers, the $Ar_2^*$ laser produces radiation with the highest photon energy of 9.8 eV. We have developed a high peak power ($\sim$MW) $Ar_2^*$ laser by use of an electron beam excitation method [9]. The electron beam excitation method, however, requires a rather large facility with a low repetition rate, resulting in limited application fields. An alternative excitation method has thus long been desired. Although several excitation methods to realize practical $Ar_2^*$ laser have been investigated, to our knowledge no evidence of the laser oscillation has been reported [10,11].

We have proposed an excitation method to demonstrate a practical $Ar_2^*$ laser using a high-intensity ultrashort pulse laser [12]. Electrons produced by a high-intensity laser will be utilized to initiate the $Ar_2^*$ production kinetics. Production of the initial electrons through an OFI process can be controlled by appropriate choice of the high-intensity laser pulse parameters [2,13]. The controlled characteristics of the laser-produced electrons should be adequate for the $Ar_2^*$ production kinetics, which may be similarly found in an electron-beam-generated plasma. In addition, we used an optical hollow fiber that was placed in a static Ar gas to guide the focused high-intensity laser pulse. By use of the gas-filled hollow fiber, an interaction length could be extended up to 50 cm, and nonlinear optical effects in free space such as self-focusing could be controlled [14,15]. It should be noted that discharge-pumped soft x-ray lasers have already utilized a similar gas-filled capillary to produce an extended pinched plasma column [3,5].

The OFI rare-gas plasma may actually have more appropriate characteristics than those found in electron-beam-generated or discharge-generated plasmas, where temporal and spatial stability of a rare-gas plasma is severely limited. The calculated initial average electron energies of the OFI Ar plasma at the intensity of $10^{15}$ W $cm^{-2}$ are 80 and 5 eV, respectively, for circularly and linearly polarized laser pulses. We, however, have found that the difference of the initial electron energy of the OFI plasma should not be reflected on the behavior of the $Ar_2^*$ production kinetics. A large excitation length (50 cm) can be provided by use of a hollow optical fiber installed in a pressurized Ar cell. To compensate for the low excitation energy ($\sim$mJ) of the ultrashort laser pulse compared with the electron-beam energy, the excitation volume should be limited for the laser-produced plasma. The use of a thin hollow optical fiber with

*Present address: Institute of Advanced Energy, Kyoto University, Uji, Kyoto 611-0011, Japan. Email address: kaku@iae.kyoto-u.ac.jp
†Email address: kubodera@opt.miyazaki-u.ac.jp

 

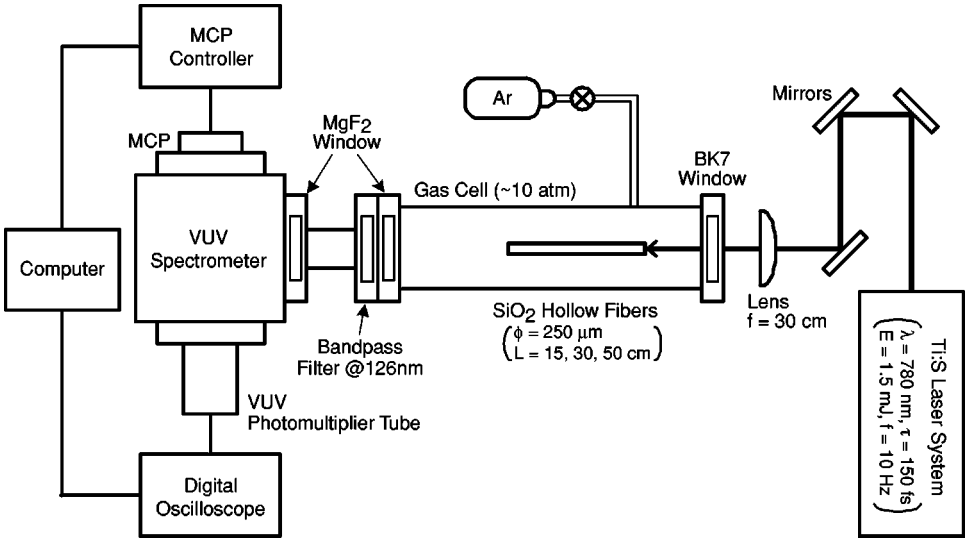


FIG. 1. Schematic diagram of the experimental apparatus.

a diameter of 250 $\mu$m is thus necessary to produce the deposited energy density of 0.2 J cm$^{-3}$ under our experimental conditions. Based on the laser energy that is dissipated in the fiber, a maximum electron density of $10^{17}$ cm$^{-3}$ is evaluated. Judging from the electron energy and density evaluated, the electrons produced by a high-intensity laser should have suitable characteristics to initiate the excimer formation kinetics.

In this paper, we report on the demonstration of the $Ar_2$* production by use of an ultrashort pulse high-intensity laser as an excitation source. $Ar_2$* emission produced by the high-intensity laser was centered at 126 nm with the spectral bandwidth of 10 nm (full width at half maximum, FWHM). Kinetic analysis revealed that the electrons produced by the high-intensity laser through an OFI process initiated the excimer production process. The pulse width of the $Ar_2$* emission was 18 ns (FWHM), which was accurately reproduced by our kinetic simulation. The $Ar_2$* emission intensity was found to be independent of the initial electron energy produced by the OFI process. The electron energy was rapidly decreased by conductive cooling in a picosecond time scale, which was adequate for the $Ar_2$* production. As a result, we have observed a small signal gain of 0.05 cm$^{-1}$ at 126 nm. The increase of the $Ar_2$* emission intensity was measured to be exp(2.5) with the fiber length of 50 cm. This excitation method, therefore, has the potential to yield a tabletop $Ar_2$* laser at 10 Hz and maybe other rare-gas excimer systems at high repetition rate.

## II. EXPERIMENTAL SETUP

Figure 1 shows a schematic diagram of the experimental apparatus. The apparatus consists of three elements: a high-intensity laser to produce an OFI plasma, a high-pressure Ar gas cell ($\sim$10 atm) where a hollow fiber is installed, and a VUV detection system. A Ti:sapphire laser at 780 nm produced the maximum output energy of 1.5 mJ with a pulse width of 150 fs at a repetition rate of 10 Hz. The laser pulse was focused inside the pressurized Ar gas cell by use of a planoconvex lens with a focal length of 30 cm. The focused laser intensity was measured to be $10^{15}$ W cm$^{-2}$ at the focus. According to the Ammosov-Delone-Krainov theory [16], this laser intensity was high enough to selectively produce singly ionized Ar ions that would relax to Ar*, a precursor of the $Ar_2$* excimer [6]. This laser intensity was necessary to yield the excimer emission. Optical hollow fibers with a diameter of 250 $\mu$m were installed in a high-pressure Ar cell. Different lengths of 15, 30, and 50 cm were chosen to guide the focused high-intensity laser pulse. The distance between the lens and the fiber entrance was kept same for all the fibers to keep the focused laser intensity constant. Time-integrated emission spectra from a fiber were detected by a VUV microchannel plate coupled to a VUV spectrometer. Typical spectral resolution was better than 0.5 nm. Emissions from an Ar plasma were observed on the high-intensity laser axis. For some measurements, a band-pass filter for the 126-nm radiation was used to minimize the intense stray light caused by the excitation laser radiation. Since the solid angles observed by the detection system were different for VUV emissions coming out of the three fibers, solid angle correction was carefully performed by measurement of the beam pattern of the visible laser radiation at the fiber exit. We assumed that the beam pattern of the VUV emission was also subject to that of the excitation laser because of the high aspect ratio of the hollow fiber. The temporal behavior of the $Ar_2$* emission at 126 nm was measured by use of a fast VUV photomultiplier tube connected to a 2-GHz sampling digital oscilloscope. All equipment was connected to a personal computer for data acquisition and processing.

## III. ARGON EXCIMER PRODUCTION BY A HIGH-INTENSITY LASER

Figure 2 shows a typical time-integrated emission spectrum of an Ar plasma produced by a high-intensity laser irradiation. The linearly polarized laser beam was focused into 10-atm Ar at the laser intensity of $10^{15}$ W cm$^{-2}$. A hollow fiber was not used for this measurement. We observed $Ar_2$* fluorescence emission centered at 126 nm, with a spectral bandwidth of 10 nm (FWHM). This bandwidth has a typical value of spontaneous emission of the $Ar_2$*, and

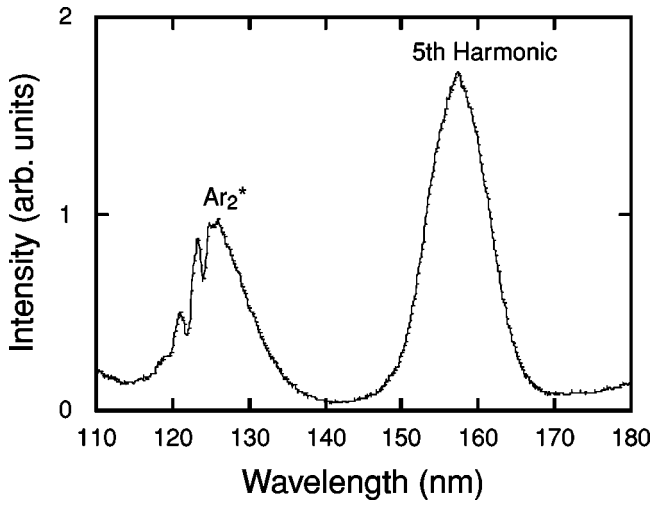


FIG. 2. Emission spectrum of $Ar_2^*$ and fifth harmonic radiation produced by high-intensity laser-produced electrons.

shows a value similar to those observed in different excitation methods [17]. The fifth-order harmonic emission of the Ti:sapphire laser was also observed at 156 nm. It should be noted that the $Ar_2^*$ spontaneous emission intensity is comparable to that of the coherent fifth harmonic emission after solid angle correction. Spectral features overlapping on the 126-nm continuum were due to absorption of impurities such as nitrogen and oxygen.

Figure 3 shows the intensities of the $Ar_2^*$ and the fifth harmonic emissions as a function of the degree of polarization of the high-intensity laser beam. A circularly polarized laser beam corresponds to the angles at 0° and 90°, and linearly polarized laser beam is at 45°. The $Ar_2^*$ emission intensity was independent of the degree of polarization. As the nonlinear optics predicts, the fifth harmonic intensity produced the maximum and minimum when the fundamental laser beam was linearly and circularly polarized, respectively. The electron energy of the OFI plasma should be very

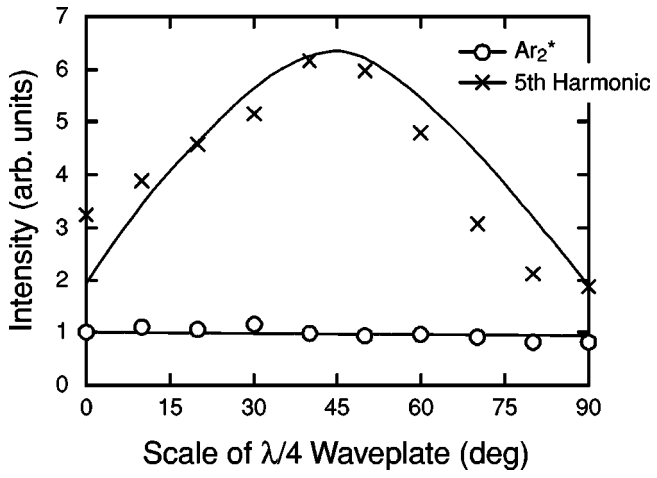


FIG. 3. $Ar_2^*$ and fifth harmonic emission intensities as a function of the degree of the laser beam polarization. Circularly and linearly polarized beams correspond to the angles of 0° or 90° and of 45°, respectively.

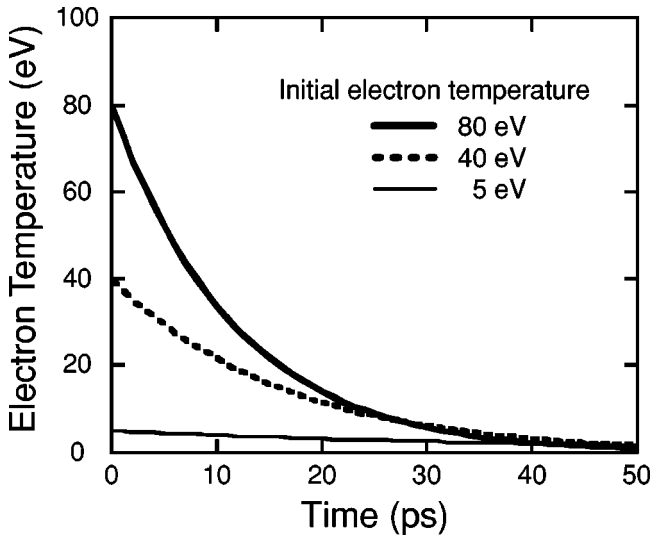


FIG. 4. Decrease of calculated electron energies by conductive cooling of electrons.

sensitive to the polarization of the laser beam [13]. The calculated average electron energies of the Ar plasma were 80 and 5 eV, respectively, for circularly and linearly polarized laser pulses under our experimental conditions. Such a large energy difference should have been reflected in the $Ar_2^*$ production kinetics. The $Ar_2^*$ emission, however, shows no dependence on the laser beam polarization, indicating the rapid electron cooling in the Ar plasma after the plasma-initiating laser pulse. In a collisionless regime, the heat flow was simply limited by the maximum flux. A fast cooling behavior of the OFI plasma has thus been evaluated numerically based on the energy transport of electrons [18,19]. The electron energy of the OFI plasma is represented as Eq. (1),

$$kT_e = (kT_e)_0 \exp\left[-\frac{2}{3}\frac{f(v_e)_0 t}{\Delta x}\right], \tag{1}$$

where $f$ is the flux limit, $(v_e)_0$ is the initial electron thermal velocity, $(kT_e)_0$ is the calculated initial electron energy, and $\Delta x$ is the radius of a plasma column.

Figure 4 represents the temporal behavior of the estimated electron energies by use of Eq. (1). Initial electron energies of 5, 40, and 80 eV were assumed with the plasma column of 30 $\mu$m, which was the same as the laser spot size. The maximum flux limit of 0.6 was used [18]. Even if the initial electron energies seem to be too high for the argon excimer production, they decrease to a few eV by the conductive cooling within 50 ps for all cases. This conductive cooling proceeds much faster than any of the other kinetics for the $Ar_2^*$ production, which occurs typically on the order of nanosecond time scale. The difference of the initial electron energy of the OFI plasma, therefore, should not be reflected on the behavior of the $Ar_2^*$ emission intensity.

The $Ar_2^*$ emission intensity at 126 nm quadratically increased with the Ar pressure as shown in Fig. 5. This pressure dependence of the $Ar_2^*$ emission intensity indicates that the excimer production kinetics is governed by the three-

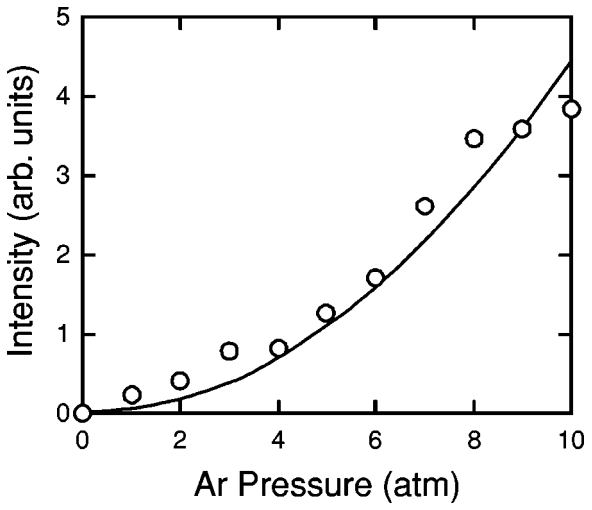


FIG. 5. Pressure dependence of $Ar_2^*$ emission intensity.

body association process such as $Ar^* + 2Ar \rightarrow Ar_2^* + Ar$. This production process becomes efficient under our high-pressure Ar conditions. It should be noted that Ar dimers played an important role in the direct production of $Ar_2^*$ in our previous observations [12,20], where dimers were prepared by a supersonic Ar gas jet. This dimerization was, however, negligible in the present static high-pressure gas condition.

Figure 6 shows the temporal behavior of the $Ar_2^*$ emission at 126 nm. The open circles represent the experimental results. The duration of the $Ar_2^*$ emission was 18 ns (FWHM). This emission time could be long enough for one to construct an optical cavity for possible laser operation. A small hump at around 50 ns is believed to be an experimental artifact. The solid curve represents the calculated temporal behavior of the $Ar_2^*$ emission by use of our kinetics code.

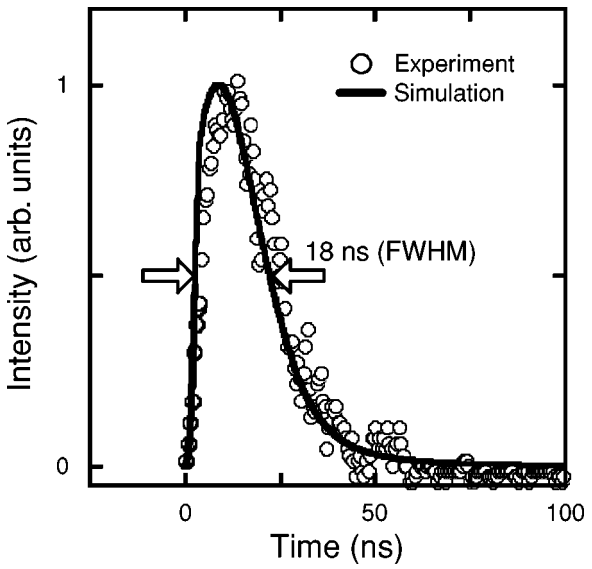


FIG. 6. Temporal behavior of $Ar_2^*$ emission. The open circles represent the experimental results. The calculated temporal behavior of the $Ar_2^*$ emission is shown by the solid curve.

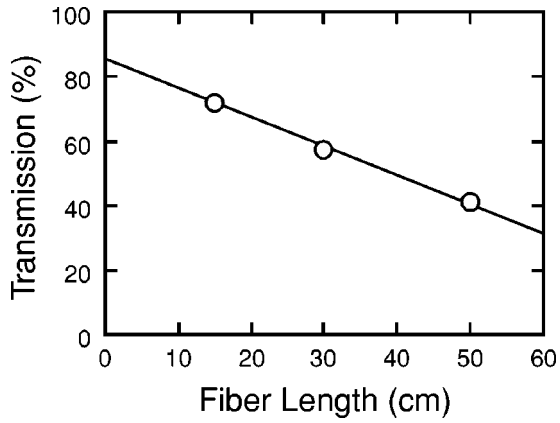


FIG. 7. Fiber length dependence of the transmission of the excitation laser energy in vacuum.

Initial electron energy and density were assumed to be 5 eV and $10^{17}$ $cm^{-3}$, respectively. The electron cooling process given by Eq. (1) was included in the calculation. The agreement verifies that the electrons produced by the high-intensity laser through an OFI process initiated the excimer formation kinetics with the assumed initial conditions. Note that no excimer emission was observed when a self-breakdown plasma was produced by a nanosecond *Q*-switched Nd:YAG (YAG, yttrium aluminum garnet) laser [12,21]. Inverse bremsstrahlung process and the following electron avalanche in a nanosecond laser-produced plasma produced highly uncontrolled plasma conditions, which was in contrast to those observed using a high-intensity laser. Coupling of nanosecond laser energy into a plasma in a gas is known to be very high, leading to a high-density, high-temperature plasma, almost behaving like a black body radiator [21,22]. Although such a high-temperature plasma cools down by fast expansion into an ambient gas, the density to maintain a gain will also decrease very rapidly, resulting in very limited plasma conditions for the optimum argon recombination scheme.

## IV. GAIN OBSERVATION AT 126 nm BY USE OF A HOLLOW FIBER

We have used optical hollow fibers to propagate a focused laser pulse, leading to the further extension of the interaction length. Figure 7 shows the plasma-initiating laser energy transmission as a function of the hollow fiber length in vacuum. The input laser energy was fixed at 1.2 mJ for all fiber lengths. Output laser energies through hollow fibers were measured by use of a power meter. The transmission linearly decreased with the fiber length by linear propagation loss, which was mainly attributed to the mode mismatch between the focused laser beam and the fiber. This propagation loss could thus have been reduced by mode matching of the loosely focused beam into a hollow fiber. The focused laser intensity, however, was not high enough to yield the excimer emission for the loosely focused beam, since the laser output energy was limited in the present condition. Based on the laser energy that is dissipated in the Ar-filled hollow fiber, the deposited energy density of 0.2 J $cm^{-3}$ was evaluated. A maximum electron density of $10^{17}$ $cm^{-3}$ was also estimated

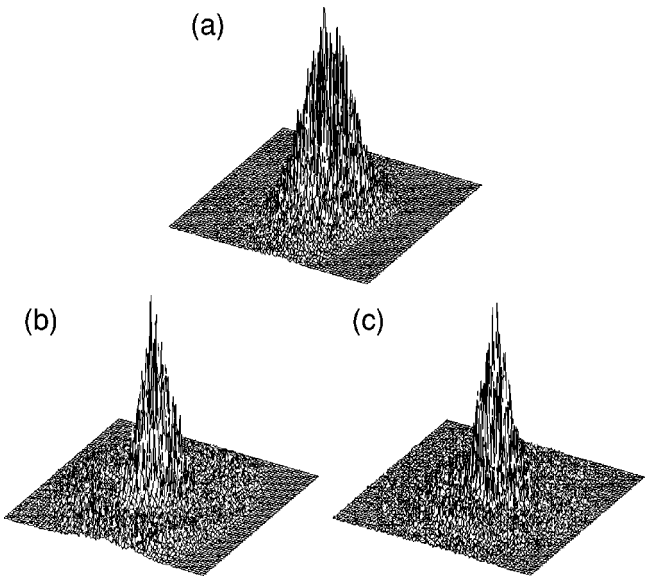


FIG. 8. Comparison of the beam profiles at the entrance and at the exit of a hollow fiber. The incident laser beam profile is shown in (a). Output beam profiles are (b) and (c). Beam profiles of (a) and (b) are taken in vacuum. Profile (c) is observed after 50-cm propagation in 10-atm Ar.

under the condition where only neutral Ar atoms were selectively ionized to singly ionized $Ar^+$ ions.

Together with the transmission characteristics of the high-intensity laser pulse in a hollow fiber, the focused laser beam patterns were measured as shown in Fig. 8. The input beam pattern was approximated as a Gaussian [Fig. 8(a)]. After the 50-cm fiber propagation, the beam patterns yielded similar Gaussian shapes both in vacuum and in 10-atm Ar, as shown in Figs. 8(b) and 8(c), respectively, indicating negligible nonlinear beam breaking phenomena in a hollow fiber. Numerically estimated pulse broadening of the excitation laser pulse was also negligible under our experimental conditions. The excitation laser intensity was thus kept constant during pulse propagation inside a fiber.

Figure 9 represents the nonlinear increase of the $Ar_2^*$ emission intensity as a function of the fiber length. Three fibers with lengths of 15, 30, and 50 cm were used. The Ar pressure was 4 atm. The laser intensity was $10^{15}$ W cm$^{-2}$, so the laser beam was focused more tightly than the diameter of the hollow fiber. This tight focusing was necessary to yield the excimer emission as described above. Based on this fiber-length dependence of the emission intensity, a small-signal gain of 0.05 cm$^{-1}$ was evaluated at the estimated deposition energy density of 0.2 J cm$^{-3}$ [23]. Note that this is, to our knowledge, the first observation of a reasonable gain coefficient at 126 nm other than the electron-beam-pumped $Ar_2^*$ laser. This gain value was approximately a third of that of the electron-beam-pumped $Ar_2^*$ laser [9], which may reflect the difference of the deposited energy density. The resulting emission intensity increase was exp(2.5) with the fiber length of 50 cm. We, however, observed no indication of the spectral narrowing of this emission, even when the fiber length was changed. Experimentally, it seems to be justified since the amplification factor (or $gL$ product) of the 126-nm emission is on the order of 10. This value may be too small to induce the spectral narrowing in the present rare-gas excimer system. The spectral narrowing of the similar excimer emission was observed only when the amplification factor of more than one hundred was realized with an appropriate optical cavity [8]. Our kinetics code also predicts that there should be very little spectral narrowing in this cavityless amplification scheme with an amplification factor of around ten.

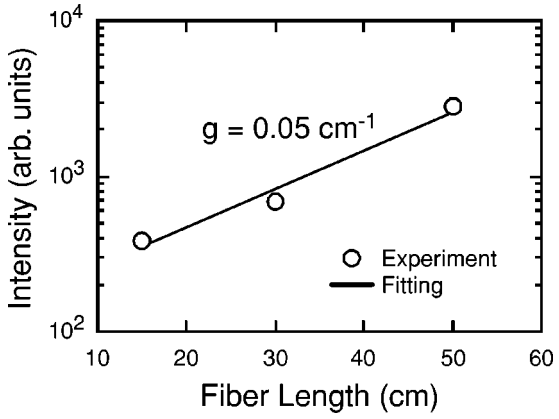


FIG. 9. Excimer emission intensity as a function of the fiber length. A small-signal gain coefficient of 0.05 cm$^{-1}$ is evaluated.

The further increase of the fiber length and the construction of an optical cavity would lead to stimulated emission at 126 nm. This high-density cold plasma production by a high-intensity laser, therefore, becomes a promising method for pumping other VUV gas lasers where optimum plasma conditions in discharge or electron-beam-generated plasmas are technically difficult to be achieved.

## V. SUMMARY

We have demonstrated the $Ar_2^*$ excimer production by use of an ultrashort-pulse high-intensity laser. The $Ar_2^*$ emission was centered at 126 nm with the spectral bandwidth of 10 nm (FWHM). Kinetic analysis revealed that the excimer production process was initiated by the electrons produced by the high-intensity laser through an OFI process. The pulse duration of the VUV fluorescence emission was 18 ns (FWHM), which was accurately reproduced by our kinetic simulation. The $Ar_2^*$ emission intensity was independent of the initial electron energy, indicating the rapid electron conductive cooling in a picosecond time scale. We have observed a small-signal gain of the $Ar_2^*$ emission by use of a hollow fiber to guide the high-intensity laser propagation in high-pressure Ar. A small-signal gain coefficient was measured to be 0.05 cm$^{-1}$ at 126 nm. The increase of the $Ar_2^*$ emission intensity was measured to be exp(2.5) with the fiber length of 50 cm. The high-density cold plasma produced by a high-intensity laser was thus adequate for the $Ar_2^*$ production and maybe for other VUV gas laser media.

**ACKNOWLEDGMENTS**

The authors acknowledge support for this work by a Grant-in-Aid for Scientific Research from the Ministry of Education, Culture, Sports, Science and Technology (MEXT) of Japan. This research was performed in collaboration with the Advanced Photon Research Center, Japan Atomic Energy Research Institute.

[1] B.E. Lemoff, G.Y. Yin, C.L. Gordon III, C.P.J. Barty, and S.E. Harris, Phys. Rev. Lett. **74**, 1574 (1995).
[2] Y. Nagata, K. Midorikawa, S. Kubodera, M. Obara, H. Tashiro, and K. Toyoda, Phys. Rev. Lett. **71**, 3774 (1993).
[3] J.J. Rocca, V. Shlyaptsev, F.G. Tomasel, O.D. Cortázar, D. Hartshorn, and J.L.A. Chilla, Phys. Rev. Lett. **73**, 2192 (1994).
[4] P.V. Nickles, V.N. Shlyaptsev, M. Kalachnikov, M. Schnürer, I. Will, and W. Sandner, Phys. Rev. Lett. **78**, 2748 (1997).
[5] K.A. Janulewicz, J.J. Rocca, F. Bortolotto, M.P. Kalachnikov, V.N. Shlyaptsev, W. Sandner, and P.V. Nickles, Phys. Rev. A **63**, 033803 (2001).
[6] M.V. McCusker, in *Excimer Lasers* (Springer-Verlag, New York, 1984).
[7] R. Sauerbrey, F. Emmert, and H. Langhoff, J. Phys. B **17**, 2057 (1984).
[8] W. Sasaki, T. Shirai, S. Kubodera, J. Kawanaka, and T. Igarashi, Opt. Lett. **26**, 503 (2001).
[9] Y. Uehara, W. Sasaki, S. Sato, E. Fujiwara, Y. Kato, M. Yamanaka, K. Tsuchida, and J. Fujita, Opt. Lett. **9**, 539 (1984).
[10] T. Efthimiopoulos, B.P. Stoicheff, and R.I. Thompson, Opt. Lett. **14**, 624 (1989).
[11] H. Ninomiya and K. Nakamura, Opt. Commun. **134**, 521 (1997).
[12] S. Kubodera, J. Kawanaka, and W. Sasaki, Opt. Commun. **182**, 407 (2000).
[13] N.H. Burnett and P.B. Corkum, J. Opt. Soc. Am. B **6**, 1195 (1989).
[14] M. Nisoli, S. De Silvestri, and O. Svelto, Opt. Lett. **22**, 522 (1997).
[15] G. Fibich and A.L. Gaeta, Opt. Lett. **25**, 335 (2000).
[16] M.V. Ammosov, N.B. Delone, and V.P. Krainov, Zh. Eksp. Teor. Fiz. **91**, 2008 (1986) [Sov. Phys. JETP **64**, 1191 (1986)].
[17] S. Kubodera, M. Kitahara, J. Kawanaka, W. Sasaki, and K. Kurosawa, Appl. Phys. Lett. **69**, 452 (1996).
[18] W.L. Kruer, *The Physics of Laser Plasma Interactions* (Addison-Wesley, Redwood City, CA, 1988).
[19] K. Midorikawa, Y. Nagata, S. Kubodera, M. Obara, and K. Toyoda, IEEE J. Sel. Top. Quantum Electron. **1**, 931 (1995).
[20] K. Mitsuhashi, T. Igarashi, M. Komori, T. Takada, E. Futagami, J. Kawanaka, S. Kubodera, K. Kurosawa, and W. Sasaki, Opt. Lett. **20**, 2423 (1995).
[21] M. Kaku, T. Yamaura, T. Higashiguchi, S. Kubodera, and W. Sasaki, Jpn. J. Appl. Phys. **42**, 3458 (2003).
[22] W.T. Silfvast and O.R. Wood II, J. Opt. Soc. Am. B **4**, 609 (1987).
[23] M. Kaku, T. Higashiguchi, S. Kubodera, and W. Sasaki, Opt. Lett. **28**, 804 (2003).